PHYSICAL REVIEW E **73**, 060501(R) (2006)

Orientation selection in lamellar phases by oscillatory shears

Zhi-Feng Huang and Jorge Viñals
McGill Institute for Advanced Materials and Department of Physics, McGill University, Montreal, QC H3A 2T8, Canada
(Received 16 January 2006; published 2 June 2006)

In order to address the selection mechanism that is responsible for the unique lamellar orientation observed in block copolymers under oscillatory shears, we use a constitutive law for the dissipative part of the stress tensor that respects the uniaxial symmetry of a lamellar phase. An interface separating two domains oriented parallel and perpendicular to the shear is shown to be hydrodynamically unstable, a situation analogous to the thin layer instability of stratified fluids under shears. The resulting secondary flows break the degeneracy between the parallel and perpendicular lamellar orientation, leading to a preferred perpendicular orientation in certain ranges of parameters of the polymer and of the shear.

DOI: 10.1103/PhysRevE.73.060501 PACS number(s): 83.50.−v, 47.20.Gv, 47.54.−r, 83.80.Uv

Oscillatory shears are often used to promote long range order in lamellar phases of block copolymers, yet the mechanisms responsible for selecting a particular lamellar orientation relative to the shear remain unknown. Ordered configurations are classified as transverse (lamellar normal parallel to the velocity field), parallel (lamellar planes parallel to the shear plane), and perpendicular (lamellar normal parallel to the vorticity direction). The latter two are shown schematically in Fig. 1. While it is generally believed that the transverse orientation is less stable under shears than the other two, the mechanisms selecting between parallel and perpendicular are not yet understood. Both are observed experimentally within ranges of parameters that depend on the architecture of the block and the shear. A possible selection mechanism based on a hydrodynamic instability of a microphase separated copolymer is presented here that can distinguish between parallel and perpendicular orientations (Fig. 1). The instability occurs at the boundary separating parallel and perpendicular regions provided that the dissipative part of the stress tensor of the copolymer is chosen to reflect the uniaxial symmetry of these broken symmetry phases. Our results rely solely on the uniaxial symmetry of lamellar phases, and therefore should generally apply to other complex fluids of the same symmetry.

Block copolymers are being extensively investigated as nanoscale templates for a wide variety of applications that include nanolithography [1–3], photonic components [4], or high density storage systems [5]. However, given the small wavelength of the microphases (tens or hundreds of angstroms), macroscopic size samples do not completely order through spontaneous self-assembly. Instead, oscillatory shears are commonly introduced in order to accelerate long range order development over the required distances (see Ref. [6] for a recent review). In practice, a variety of lamellar orientations are observed [6–11]. The first theoretical analysis of the orientation selection in block copolymers was conducted in the vicinity of the order-disorder transition of the copolymer, and addressed the effect of a *steady* shear on the growth of critical fluctuations [12]. Fluctuations along the perpendicular orientation were shown to be less suppressed by the shear, and hence it was argued that this orientation would be selected. Consideration was later given to anisotropic viscosities of smectics, which led to different relative stabilities of uniform parallel and perpendicular configurations due to the different effects of thermal fluctuations on each orientation [13]. Later work focused on the role played by a viscosity contrast between the microphases [14], and showed that the perpendicular alignment dominates at high shear rates, and parallel otherwise. However, existing experimental phenomenology concerning orientation selection [6–11] is far more complex than these analyses would suggest. The analysis that we present here does not rely on fluctuation effects near critical points, allows for oscillatory shears, and explicitly incorporates hydrodynamic effects resulting from a viscosity contrast between lamellar phases of different orientations, thus overcoming the limitations of previous treatments.

The experimentally relevant range of shear frequencies is well below the inverse characteristic relaxation times of the polymer chains, and hence a reduced description in terms of the monomer volume fraction is adopted [14–16]. According to this description, the lamellar phase response is solidlike or elastic for perturbations directed along the lamellas normal, and fluidlike or viscous on the lamellar plane. In the limit of vanishing frequency, the viscous part of the response has been assumed to be Newtonian with uniform shear viscosity,

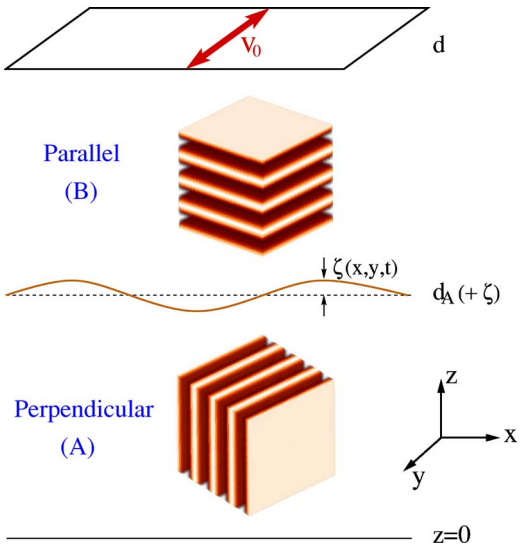

FIG. 1. (Color online) Schematic representation of a parallel and/or perpendicular configuration being sheared along $\hat{y}$.

and therefore parallel and perpendicular orientations are degenerate and unmodified by the shear. We address below the consequences of what we believe is the leading deviation away from the Newtonian response in the limits of low frequency and characteristic flow scale much longer than the lamellar spacing: the viscous stress tensor of a lamellar phase is, by reason of symmetry, the same as that of any other uniaxial phase (e.g., a nematic liquid crystal [17,18]). The slowly varying local wave vector of the lamellas plays a role analogous to that of the director in a nematic. The rest of this paper is devoted to the study of the effect of this assumption on the hydrodynamic stability of the configuration shown in Fig. 1.

We assume that the dissipative part of the linear stress tensor is that of a uniaxial, incompressible phase [18],

$$\sigma_{ij}^D = \eta D_{ij} + \alpha_1 \hat{n}_i \hat{n}_j \hat{n}_k \hat{n}_l D_{kl} + \alpha_{56}(\hat{n}_i \hat{n}_k D_{jk} + \hat{n}_j \hat{n}_k D_{ik}) \quad (1)$$

with $i,j,k,l=x,y,z$, $D_{ij}=\partial_i v_j+\partial_j v_i$ with v_i the local velocity field, and $\hat{\mathbf{n}}=(\hat{n}_x,\hat{n}_y,\hat{n}_z)$ denoting the *slowly varying* normal to the lamellar planes. The Newtonian viscosity is η, and α_1 and α_{56} are two independent viscosity coefficients. The dynamic viscosity η' ($\eta'=G''/\omega$, with G'' the loss modulus and ω the shear frequency) is $\eta'=\eta$ for a fully ordered perpendicular configuration [$\hat{\mathbf{n}}=(1,0,0)$], and $\eta'=\eta+\alpha_{56}$ for a parallel orientation [$\hat{\mathbf{n}}=(0,0,1)$]. This model is consistent with low frequency rheology in poly(ethylene-propylene)-poly(ethylethylene) (PEP-PEE) diblocks showing $\eta'_{\mathrm{par}}>\eta'_{\mathrm{perp}}$ [7] if $\alpha_{56}>0$, and with poly(styrene)-poly(isoprene) (PS-PI) diblocks $\eta'_{\mathrm{par}}<\eta'_{\mathrm{perp}}$ [11] if $\alpha_{56}<0$. Given this assumption, the effective dynamic viscosity in the two domain configurations of Fig. 1 would be different in each domain. It is known that the analogous configuration for the case of two Newtonian fluids of different viscosity is unstable both for steady [19,20] and oscillatory [21] shears. We describe below the extension of these results to uniaxial phases in the limit of small but nonzero Reynolds number flows. Note that the focus here is on low enough shear frequencies for which the polymer chains remain relaxed and molecular deformations and block details play a secondary role [6]; therefore, our results below should hold for copolymers of different numbers of blocks.

We consider a base state involving perpendicular (A) and parallel (B) regions separated by a planar surface, subjected to an imposed shear $\mathbf{v}_0=\gamma\omega d\cos(\omega t)\hat{\mathbf{y}}$ at $z=d$, and $\mathbf{v}_0=0$ at $z=0$ (Fig. 1), with γ the shear amplitude and d the system thickness. The resulting velocity field $\mathbf{v}_{A,B}=(0,V_{A,B},0)$ is the same as that of two superposed Newtonian fluids with viscosities $\mu_A=\eta$ and $\mu_B=\eta+\alpha_{56}$. We then consider a small perturbation of the domain boundary as shown in Fig. 1, and write the velocity fields in A and B as $v_i^{A,B}=V_{A,B}\delta_{iy}+u_i^{A,B}$ ($i=x,y,z$). By expanding $u_i^{A,B}=\Sigma_{q_x,q_y}\hat{u}_i^{A,B}(q_x,q_y,z,t)\exp[i(q_x x+q_y y)]$, substituting into the modified Navier Stokes equation that results from the choice of Eq. (1), linearizing, and eliminating pressure and $\hat{u}_y$, we find

$$\begin{aligned}\mathrm{Re}[&(\partial_t+iq_yV_A)(\partial_z^2-q^2)\hat{u}_z^A-iq_y(\partial_z^2V_A)\hat{u}_z^A]\\&=(\partial_z^2-q^2)^2\hat{u}_z^A-\alpha_{56}q_x^2(\partial_z^2-q^2)\hat{u}_z^A\\&\quad+iq_x[2\alpha_1q_x^2-\alpha_{56}(\partial_z^2-q^2)]\partial_z\hat{u}_x^A,\end{aligned} \quad (2)$$

$$\begin{aligned}\mathrm{Re}[&\partial_t(\partial_z^2-q^2)\hat{u}_x^A+iq_y(\partial_z^2-q^2)(V_A\hat{u}_x^A)+2q_xq_y(\partial_zV_A)\hat{u}_z^A]\\&=(1+\alpha_{56})(\partial_z^2-q^2)^2\hat{u}_x^A-2\alpha_1q_x^2(\partial_z^2-q_y^2)\hat{u}_x^A,\end{aligned} \quad (3)$$

for the perpendicular domain A ($0\le z\le d_A$). Here $q^2=q_x^2+q_y^2$ and $\mathrm{Re}=\rho\omega d^2/\eta$ is the Reynolds number, with ρ the copolymer density. Similarly

$$\begin{aligned}\mathrm{Re}[&(\partial_t+iq_yV_B)(\partial_z^2-q^2)\hat{u}_z^B-iq_y(\partial_z^2V_B)\hat{u}_z^B]\\&=(1+\alpha_{56})(\partial_z^2-q^2)^2\hat{u}_z^B-2\alpha_1q^2\partial_z^2\hat{u}_z^B,\end{aligned} \quad (4)$$

$$\begin{aligned}\mathrm{Re}[&\partial_t(\partial_z^2-q^2)\hat{u}_x^B+iq_y(\partial_z^2-q^2)(V_B\hat{u}_x^B)+2q_xq_y(\partial_zV_B)\hat{u}_z^B]\\&=(\partial_z^2-q^2)^2\hat{u}_x^B+\alpha_{56}(\partial_z^2-q^2)(\partial_z^2\hat{u}_x^B-iq_x\partial_z\hat{u}_z^B)\\&\quad-2iq_x\alpha_1\partial_z^3\hat{u}_z^B,\end{aligned} \quad (5)$$

for the parallel region B ($d_A\le z\le d$). All quantities have been made dimensionless by a length scale d, a time scale ω^{-1}, and rescaling viscosities by η, i.e., $\alpha_1\to\alpha_1/\eta$ and $\alpha_{56}\to\alpha_{56}/\eta$ ($\mu_A=1$, $\mu_B=1+\alpha_{56}$). Rigid boundary conditions are used on the planes $z=0$ and $z=d$ ($d=1$ after rescaling). At the interface $z=d_A+\zeta(x,y,t)$ we have $\mathbf{v}^A=\mathbf{v}^B$, and $(\sigma_{ij}^B-\sigma_{ij}^A)\hat{n}_j=-\Gamma'(\partial_x^2+\partial_y^2)\zeta\hat{n}_i\delta_{iz}$ with $\Gamma'=\Gamma/(\eta\omega d)$ and Γ the interfacial tension. Also, the kinematic boundary condition for the interface is $(\partial_t+\mathbf{v}^B\cdot\boldsymbol{\nabla})\zeta=v_z^B$.

Equations (2)–(5) are similar to the Orr-Sommerfeld equation for the Newtonian case [19–21], except that x and z velocity fields are now coupled (except at $q_x=0$). The solution can be found by writing $\hat{u}_{z,x}^{A,B}=\exp(\sigma t)\phi_{z,x}^{A,B}$ and $\hat{\zeta}=\exp(\sigma t)h$, with $\hat{\zeta}$ the Fourier transform of ζ, and σ the Floquet exponent yielding the perturbation growth rate [coefficients in Eqs. (2)–(5) proportional to $V_{A,B}$ are periodic in time].

For typical block copolymers, $\rho\sim1$ g cm^{-3}, $d\sim1$ cm, and $\eta\sim10^4$–10^6 P, resulting in $\mathrm{Re}/\omega=10^{-4}$–$10^{-6}$ s. Hence, $\mathrm{Re}\ll1$ for the frequencies of interest. We further expand the velocity, interfacial functions $\phi_{z,x}^{A,B}$, h, as well as the Floquet exponent σ in powers of Re, and solve Eqs. (2)–(5) order by order. In the limit $\mathrm{Re}\to0$ while keeping the surface tension Γ' finite, we find $\sigma=f_{z0}^B(q_x,q_y)\Gamma'$, with $f_{z0}^B<0$ for all wave numbers q_x and q_y. Hence the interface is stable, indicating coexistence of parallel and perpendicular orientations in this limit.

The situation is different for small but finite values of Re. In this case we need to address the order of Γ' as well. Typical values of $\Gamma\sim1$ dyn/cm lead to $\Gamma'\omega=10^{-4}$–10^{-6} s^{-1}. Given that $\mathrm{Re}/\omega=10^{-4}$–$10^{-6}$ s, and that $\omega\sim1$ s^{-1} in typical experiments, we consider the distinguished limit $\Gamma'=O(\mathrm{Re})$. Writing $\Gamma'=\Gamma_1\mathrm{Re}$, and $\sigma=\sigma_1\mathrm{Re}$, we find

$$\sigma_1=f_{z0}^B(q_x,q_y)\Gamma_1+\tfrac{1}{2}\delta^2\gamma^2f_{z1}^B(q_x,q_y). \quad (6)$$

Here $\delta=m\lambda_0$ is proportional to the viscosity contrast $m=\mu_A/\mu_B$, with $\lambda_0=(d_A+md_B)^{-1}$, $d_B=d-d_A$, and the function $f_{z1}^B(q_x,q_y)$ depends on the system parameters α_1, α_{56}, and on d_A, but not on the shear parameters γ and ω. Whereas f_{z0}^B is always negative, f_{z1}^B can be positive so that Eq. (6) illustrates the competition between the stabilizing effect of surface tension and the destabilizing effect of the imposed

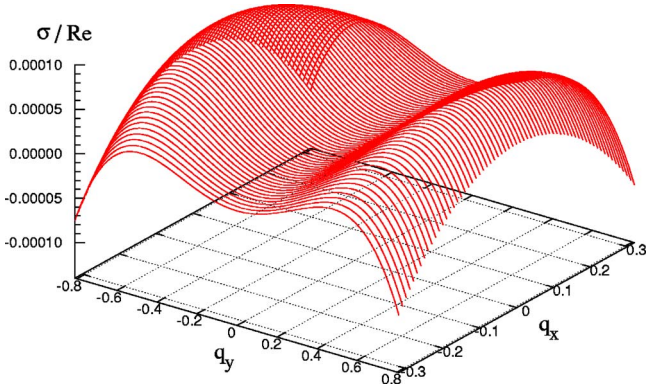

FIG. 2. (Color online) Growth rate σ/Re as a function of wave numbers q_x and q_y, for $\alpha_1=1$, $\alpha_{56}=-0.9$, $\gamma=1$, $\mathrm{Re}=5\times10^{-4}$, and $d_A=\frac{1}{2}$. The maximum growth rate is found at $q_x^{\max}=0$, $q_y^{\max}=\pm0.61$.

shear flow. Note that $\Gamma_1=1/\mathrm{We}=\theta\omega^{-2}$, with We the Weber number and $\theta=\Gamma/(\rho d^3)$. Thus $\sigma_1=\sigma_1(\gamma^2,\omega^{-2})$, and the instability is increased at large shear amplitudes and frequencies.

Typical results for σ as a function of wave vectors are shown in Fig. 2. Unstable wave vectors are near $q_x=0$. This indicates the absence of interfacial modulation along the x direction (the transverse direction for perpendicular lamellas), and $u_x=0$ for the associated velocity perturbations. We have repeated the calculations for different ranges of parameters, and found similar results for both σ and velocity perturbations.

Based on these results, further progress in determining the stability boundary can be made by examining only long waves along the y direction (with $q=q_y$). Equation (6) is expanded as $f_{z0}^B=-f_0q^4+O(q^6)$, $f_{z1}^B=f_1q^2+f_2q^4+O(q^6)$, so that the Floquet exponent is given by

$$\sigma_1=\tfrac{1}{2}\delta^2\gamma^2f_1q^2-\left(\theta f_0\omega^{-2}-\tfrac{1}{2}\delta^2\gamma^2f_2\right)q^4, \qquad (7)$$

where $f_0>0$ always, as noted above. Both $f_1=f_1(\alpha_{56},d_A)$ and $f_2=f_2(\alpha_1,\alpha_{56},d_A)$ are complicated but known functions of their arguments. For small q stability is determined by the sign of f_1, which depends on α_{56} and layer thickness d_A but is independent of shear parameters. The calculated stability diagram in the $(d_A/d_B,\mu_B)$ plane $(\mu_B=1+\alpha_{56})$ is shown in Fig. 3. Note the symmetry under $d_A/d_B\to(d_A/d_B)^{-1}$ and $\mu_B\to\mu_B^{-1}$ which suggests that this instability is related to the known two fluid instability produced by a viscosity stratification [20]: instability occurs when the thinner domain is more viscous. In the present case, however, viscosity contrast between the domains is not caused by fluid stratification, but rather because of the effective viscosity contrast between lamellas of different orientations.

The stability analysis discussed thus far is purely of hydrodynamic nature, but can be used to argue that the growth of unstable modes above threshold leads to an orientation selection. As can be seen from Fig. 1, parallel lamellas are marginal to velocity fields along x and y directions, but will be compressed or expanded by nonuniform flows along the z direction. Conversely, perpendicular lamellas will be distorted by nonuniform flows along x, but not by flows along

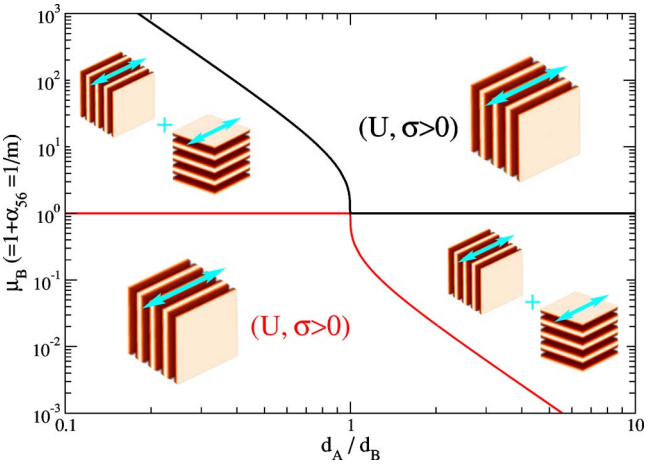

FIG. 3. (Color online) Orientation selection for uniaxial systems under oscillatory shears as a function of the layer thickness ratio and viscosity contrast. (U, $\sigma>0$) denotes the range in which the parallel orientation is unstable, leading to the selection of the perpendicular orientation.

either y or z. Since the instability mode is dominated by a velocity field along z, it will lead to weak and oscillatory compression and expansion of the parallel region, while leaving the perpendicular lamellas unaffected. The response of an interface separating two lamellar phases, subjected to periodic expansion and compression and the other marginal, has already been addressed in Ref. [22]. We showed that the overall free energy of the system is reduced by the motion of the interface towards the distorted phase (which is storing elastic energy during each cycle of the shear) or, in the present case, toward the parallel region. In summary, Fig. 3 shows the regions of parameters in which parallel and perpendicular layers would coexist, and those in which the layer of perpendicular orientation would grow at the expense of the parallel layer. It would be interesting to test our predictions by examining a system comprising only two layers of different orientations and with varying ratios d_A/d_B to directly address the stability of the configuration under shears, and to indirectly measure the coefficient α_{56} from the location of the instability threshold.

Experiments addressing orientation selection always involve coarsening of polycrystalline samples with a distribution of grain sizes, and hence a range of ratios d_A/d_B, and a distribution of orientations. It is generally argued that lamellar domains with local wave vectors not on the parallel and/or perpendicular plane will be eliminated from the distribution rather quickly, and hence that the selection of a final orientation will be determined by the competition between parallel and perpendicular domains. Generally speaking, our results imply selection of the perpendicular orientation for finite shear frequencies and $\alpha_{56}>0$, the latter case appropriate for PEP-PEE but not PS-PI blocks if our assumption in Eq. (1) holds. If $\alpha_{56}<0$, Fig. 3 would suggest that a smaller than average layer of perpendicular orientation first grows at the expense of neighboring parallel layers. Following this initial coarsening in which d_A/d_B increases in time, the stability boundary in this figure would be reached. It is difficult to assess in this case the impact of other dynamical factors

affecting coarsening such as the effect of an already moving boundary and the concomitant flows, or spatial correlations built into the distribution of orientations following this intermediate coarsening [23]. In summary, if $\alpha_{56}<0$, as well as in the limit of $\mathrm{Re}\to 0$, our study indicates coexistence of parallel and perpendicular domains, not inconsistently with experiments addressing orientation selection that indicate dependence on processing history or experimental details [6,8,9] (e.g., quenched or annealed history of the sample, and the starting time of shear alignment).

Once within the region of instability, it is instructive to analyze the dependence of the growth rate of the most unstable perturbation on the parameters of the shear. This growth rate is given by $\sigma_1^{\max}=(\delta^4 f_1^2/16f')\gamma^4\omega^2$, with $f'=\theta f_0-\delta^2 f_2\gamma^2\omega^2/2$, and the corresponding most unstable wave number is $q_{\max}=\delta(f_1/f')^{1/2}\gamma\omega/2$, both of which increase with shear amplitude and frequency. By noting that $\sigma_1^{\max}=\sigma_{\max}/\mathrm{Re}=\sigma_{\max}\eta/(\rho d^2\omega)$, and that usually $\sigma_{\max}\ll(\rho d^2\delta^2 f_1^2/8|f_2|\,\eta)\gamma^2\omega$ for small enough $\sigma_{\max}$, we find the maximum growth rate to be given by

$$\sigma_{\max}=\frac{\rho d^2\delta^4 f_1^2}{16\theta f_0\eta}\gamma^4\omega^3. \tag{8}$$

Therefore, the perturbation growth for a given block copolymer is constant along the line $\gamma\omega^{3/4}=$const. To our knowledge, the only experimental determination of the boundary in a parameter space separating regions in which parallel or perpendicular lamellas are selected has been given for PS-PI copolymers [9,10]. From a limited data set, it was approximated by $\gamma\omega=$ const. Since it is not inconceivable that the experimentally determined boundary does not correspond to the true stability boundary, but rather to the line in which $\sigma_{\max}$ becomes experimentally observable [24], it would be desirable to conduct the experiment in a block copolymer with $\alpha_{56}>0$.

In summary, by assuming that the dissipative part of the linear stress tensor of a block copolymer has to respect the broken symmetry of uniaxial lamellar phases, we have obtained a finite wavelength hydrodynamic instability of the interface separating lamellas of parallel and perpendicular orientations under an imposed oscillatory shear. The instability leads to nonuniform secondary flows, which would favor the perpendicular orientation in large regions of parameter space. Since our results follow from the symmetry of the lamellar phases, we would expect them to hold in other complex fluids of the same symmetry.

This research has been supported by NSF under Grant No. DMR-0100903 and by NSERC Canada.

[1] C. Harrison *et al.*, Science **290**, 1558 (2000).
[2] C. T. Black and O. Bezencenet, IEEE Trans. Nanotechnol. **3**, 412 (2004).
[3] C. T. Black, Appl. Phys. Lett. **87**, 163116 (2005).
[4] A. Urbas, Y. Fink, and E. L. Thomas, Macromolecules **32**, 4748 (1999).
[5] T. Thurn-Albrecht *et al.*, Science **290**, 2126 (2000).
[6] R. G. Larson, *The Structure and Rheology of Complex Fluids* (Oxford University Press, New York, 1999).
[7] K. A. Koppi *et al.*, J. Phys. II **2**, 1941 (1992).
[8] S. S. Patel, R. G. Larson, K. I. Winey, and H. Watanabe, Macromolecules **28**, 4313 (1995).
[9] D. Maring and U. Wiesner, Macromolecules **30**, 660 (1997).
[10] H. Leist, D. Maring, T. Thurn-Albrecht, and U. Wiesner, J. Chem. Phys. **110**, 8225 (1999).
[11] Z. R. Chen and J. A. Kornfield, Polymer **39**, 4679 (1998).
[12] M. E. Cates and S. T. Milner, Phys. Rev. Lett. **62**, 1856 (1989).
[13] M. Goulian and S. T. Milner, Phys. Rev. Lett. **74**, 1775 (1995).
[14] G. H. Fredrickson, J. Rheol. **38**, 1045 (1994).
[15] L. Leibler, Macromolecules **13**, 1602 (1980).
[16] T. Ohta and K. Kawasaki, Macromolecules **19**, 2621 (1986).
[17] P. C. Martin, O. Parodi, and P. S. Pershan, Phys. Rev. A **6**, 2401 (1972).
[18] P. G. de Gennes and J. Prost, *The Physics of Liquid Crystals* (Clarendon, Oxford, 1993).
[19] C. S. Yih, J. Fluid Mech. **27**, 337 (1967).
[20] A. P. Hooper, Phys. Fluids **28**, 1613 (1985).
[21] M. R. King, D. T. Leighton, Jr., and M. J. McCready, Phys. Fluids **11**, 833 (1999).
[22] Z.-F. Huang, F. Drolet, and J. Viñals, Macromolecules **36**, 9622 (2003).
[23] W. W. Mullins and J. Viñals, Acta Metall. Mater. **41**, 1359 (1993).
[24] An analogous situation would be the determination of the cloud point in nucleation studies.